Development of an Aircraft and Landing Gears Model with Steering System in Modelica-Dymola

Gianluca Verzichelli
Airbus UK Ltd.
BS99 7AR, Filton. United Kingdom
gianluca.verzichelli@airbus.com

Abstract

This paper describes one of the first uses of Modelica, with Dymola, for modelling and simulation activities of landing gears in Airbus. The application of Dymola was for the development of a model of the whole Aircraft and the auxiliary and main landing gears, including tires, wheels, oleo-pneumatic shock absorbers, airframe, etc.
The suitability of Modelica for describing model at system level has been exploited. In this case, it has provided steering functions for the whole Aircraft, with the development of the Nose and Body Wheel Hydraulics Steering System connected to the mechanical domain. Furthermore, most of the electrical components, part of the Control and Monitoring System of the Aircraft, have been taking into account, so that the interaction between the electrical, hydraulics and mechanical domains forms a close link using one modelling language. The model has been developed using mainly the free library *Mechanics* and the commercial library *HyLib*.
Keywords: aircraft; landing gear; steering system; simulation; modelling.

1 Introduction

Over the last three decades, civil aircraft systems have become progressively more integrated, encompassing several different domains: structure, power, control and software. In a such tightly coupled environment the use of one modeling and simulation language like Modelica, can provide tangible advantages for the engineers. In particular, it can decrease the lead-time to develop several *ready-to-use* architectures of the Aircraft model, with different levels of detail, so that the engineers can investigate many more *what-if* strategies with high level of accuracy of the analysis, thus minimizing the risks of the *design-build-test-fix* cycle, which is an expensive, uncompetitive, unpredictable – and ultimately prone to failures, paradigm of product development.

2 Aircraft Library

The following sections highlight the main features of the sub-models developed for the Aircraft Library. Any of them can be placed in a super-model to create a detailed architecture of a desired aircraft which then can be tested under the foreseen simulated operative conditions, see Figure 1.

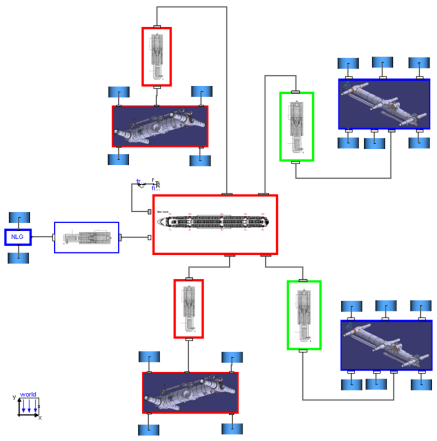

Figure 1: Snapshot of the full model in Dymola

2.1 Airframe Model

The Airframe Model contains the mass, inertia tensor and the main geometrical characteristics of the Aircraft (A/C) like wheelbase, track, etc. The mass is lumped and concentrated at the Centre of Gravity (CG) location and the inertia tensor is calculated with respect to the CG. The user can define the position of the CG (yellow sphere) with respect to the Mean Aerodynamic Chord (MAC) of the A/C (purple segment),

typically between 35% and 42% of the MAC, see Figure 2.

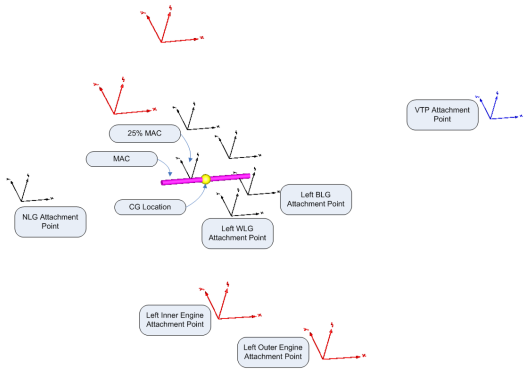

Figure 2: Airframe Model in Dymola with parameterized attachment points

In addition the user can define the attachment points of the Nose, Wing, Body Landing Gears, the Engines and the Vertical Tail Plane Pressure Centre with respect to the Aircraft Datum, see Figure 3.

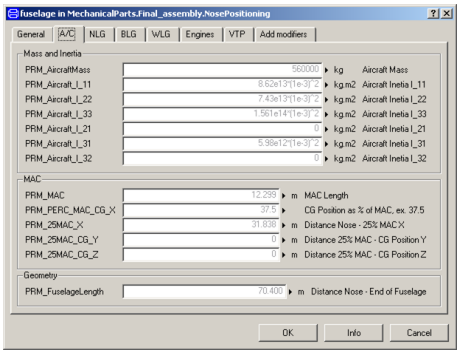

Figure 3: GUI for definition of the Airframe Model main parameters

The approach to lump the whole mass and inertia tensor of the A/C at the CG location is quite common and straightforward, it is also typical of the models built with a top-down approach. This method implies an extensive use of the *FixedTranslation* Block, with no mass and inertia: the only mass and inertia are in the Airframe Model. Though this is theoretically correct, Modelica could experience problems solving the equation of motions in all the cases where there is a *local* translation or rotation of two parts: for instance, the rotation of the steerable aft axle of the Body Landing Gear with respect to the Bogie. This method is also unadvisable in all those cases when the models are built with a bottom-up approach (many sub-models which will be used to develop a top level model): in these cases, each part of the sub-models should have its own correct, or at least realistic, mass and inertia, so that the sub-model can be verified and validated in isolation.

2.2 Shock Absorber Model

The Shock Absorber is represented by means of an oleo-pneumatic suspension model. Its characteristics vary with relative displacement, velocity and direction of travel of the sliding cylinder with respect to the outer cylinder. The model contains characteristics for stiffness and damping for each of the landing gears as supplied by the vendors (polytropic dynamic curves). Stiffness force is calculated as a function of oleo extension displacement via evaluation of spring stiffness curves, see Figure 4.
Damping force is calculated as a function of oleo extension displacement, the rate of change of oleo extension displacement and oleo extension displacement direction. To achieve this, two damping coefficient curves are used, one defining the compression stroke coefficient against oleo extension displacement and one defining rebound stroke, see Figure 5 and Figure 6. Oleo damping force is then calculated by multiplying this coefficient by velocity squared.
At the top-level, the user can define the rake angle of the shock absorber and other key characteristics (maximum stroke, sliding cylinder length, etc.).

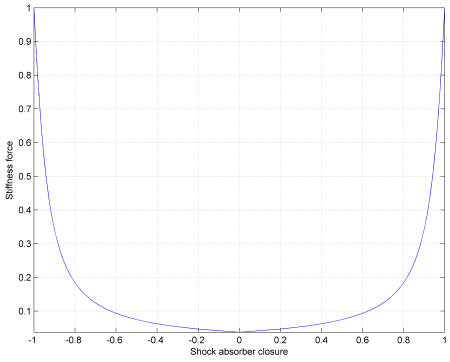

Figure 4: Stiffness force vs. shock absorber closure at 20° Celsius (Normalized)

2.3 Bogie Model

The main functionality of the Bogie model is to provide attachment points for the wheels and the bottom of the shock absorber so to create a correct load path distribution of the weight of the A/C on the ground. The user can choose between a Dual, a Dual Tandem a Tri-Twin Tandem Bogie. Obviously other types of

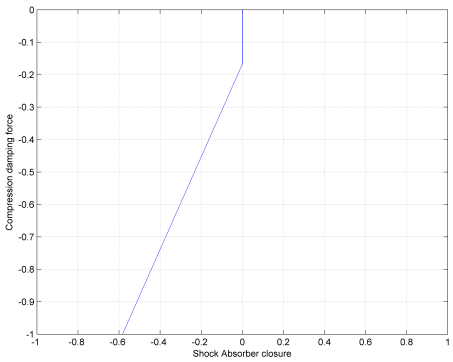

Figure 5: Compression damping force vs. shock absorber closure at 20° Celsius (Normalized)

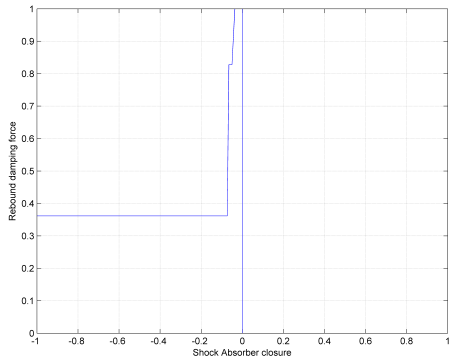

Figure 6: Rebound damping force vs. shock absorber closure at 20° Celsius (Normalized)

Landing Gears Wheel Layouts model can be easily developed: Dual Twin, Dual Twin Tandem, etc. In the case of the Body Wheel Steering (BWS), the aft axle is steerable, see Figure 7, so the model provides extra functionalities: these are explained in § 2.3.1.
The user can define the main geometrical characteristics like track and wheelbase and whether consider it as massless and with zero inertia or not.

2.3.1 Body Landing Gear Model

The Body Landing Gear (BLG) Model has extra functionality because of its characteristic of having the aft axle steerable. It includes the *LineForceWithTwoMasses* Block for the inclusion of the steering actuator and lock actuator characteristics (lumped masses of cylinder and piston) and connection to the hydraulics actuator of the Steering System Model, as well as Return springs. In addition, a *brake* Block has been used to simulate the status of locked condition of the aft axle. When the Avionic System commands to lock the aft axle, supposed to be initially unlocked, a command

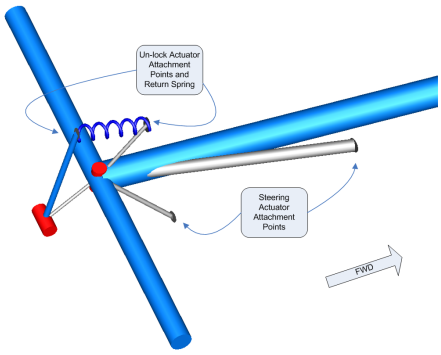

Figure 7: Tri-Twin Tandem Bogie Model with steerable aft axle and lock system

to retract the lock actuator is sent.
The Lock system uses a wedge beam that pivots a one end attached to the bogie whilst the other end is attached to the locking actuator, see Figures 7 and 8.

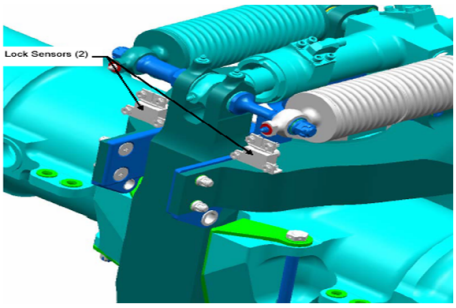

Figure 8: Lock System

As the lock beam is drawn towards the aft axle via the Return springs (retraction of the lock actuator) it engages its wedge into a V-shape aperture in the axle causing it to be locked. As the lock beam is deployed away from the aft axle (extension of the lock actuator) the wedge becomes free from the aperture in the axle allowing the axle to rotate freely. The return springs not only reduce the closing force needed to lock the locking wedge but also maintain the locking wedge in its closed position.
At the moment, given a certain part, Modelica does not recognize the surface of it but only *frame a* and *frame b*, together with the position of the CG with respect to *frame a*, the mass and inertia tensor of the part. So the simulation of surfaces contact/collision is not possible unless the point, or points, of contact/collision remain known during the whole simulation.

2.4 Tyre Model

The modelling and simulation activity of a tyre, and in particular of an aircraft tyre – subject to higher slip

angles with respect to automotive tyres – represents a difficult task. Many different tyre models have been developed in Modelica: Magic Formula model, Rill Model, Brush Model, see [1], with different level of accuracy and computational effort. The model developed for the Aircraft Library represents a good compromise between accuracy and simulation time and it seems to be suitable for on ground manoeuvrability studies. Obviously, thanks to the modularity development feature of the Modelica language, when a more detailed model of the tyre will be developed, this can be easily and quickly implemented in the full A/C model.
The model developed makes use mainly of look up tables with empirical data extracted from tyre suppliers manufacturers. The model calculates Lateral Slip Angle, Side and Drag Forces, Vertical Reaction and Self Aligning Torque. The point of application of the Side, Drag Forces and Self Aligning Torque is fixed and it is coincident with the vertical projection of the axle hub at a vertical distance equal to deformed radius of the tyre. The runway and taxiway are assumed to be flat and the camber angle is neglected. The model allows the user to chose the value of the coefficient of rolling resistance, the tyre deformed radius, the inflation pressure, the tyre damping coefficient, the mass and inertia of the tyre.

2.4.1 Lateral Slip Angle Computation

The Lateral Slip Angle is the angle formed by the plane of rotation of the wheel and the tangent to the wheel's path, see Figure 9. Mathematically can be expressed as:

$$\alpha_y = \arctan(V_y/V_x) \tag{1}$$

where V_y and V_x are the velocities of the footprint of the resultant of the pressure distribution forces between tyre and ground. The model uses the simplified assumption explained in § 2.4, so it assumes that there is no elastic deformation of the tyre belt for the computation of the lateral slip angle.

The value of (1), computed by the model, is different from zero only when there is contact between tyre and ground and the lateral and longitudinal velocities of the tyre footprint are above a certain threshold. In addition, the model assumes an instantaneous development of steady state reaction forces and momentum.

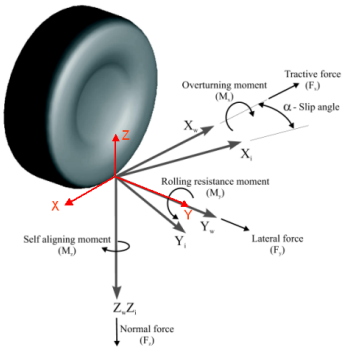

Figure 9: Tyre axis system as defined by the SAE

2.4.2 Vertical Reaction Computation

The Vertical Reaction is calculated by means of a non-linear spring behavior using the following equation:

$$Max(0,\ k \cdot (q - q_0)^e - c \cdot \dot{q}) \tag{2}$$

where k is the stiffness coefficient, c is the damping coefficient, e is a coefficient depending on the type of material, q is the actual displacement variable, q_0 is the tyre deformed radius, $\dot{q}$ is the actual velocity variable. Another model computes the dynamic Vertical Reaction of the tyre using (2) but substituting the stiffness behavior $k \cdot (q - q_0)^e$, with the look-up table of Figure 10, which takes into account the inflation pressure and the actual deflection of the tyre.

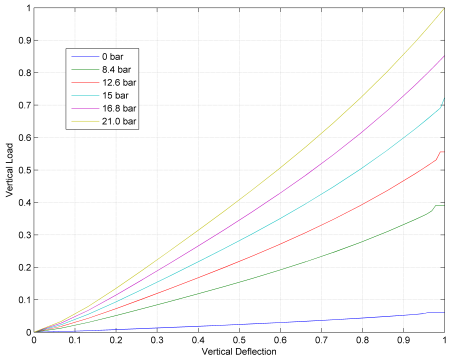

Figure 10: Dynamic Vertical Load vs. Vertical Deflection for different Inflation Pressures (Normalized)

The user can choose between the two different methods of computation because the model has been made *replaceable*.
The Vertical Reaction sustained by each tyre and the lateral slip angle are used to calculate the tyre forces and torques as explained in § 2.4.3.

2.4.3 Side, Drag Forces and Self Aligning Torque Computation

The equations which compute the drag and side forces are as follow:

$$D = \mu_R \cdot F_z + D' cos(\alpha_y) - S' sin(\alpha_y) \quad (3)$$

$$S = S' cos(\alpha_y) + D' sin(\alpha_y) \quad (4)$$

where μ_R is the rolling friction coefficient, F_z is the Vertical Load, D' and S' are the drag and side forces resolved in the wheel plane reference system and α_y is the slip angle. Notably, there is no need to manipulate them if α_y changes sign, because of the trigonometric functions *sin* and *cos* and the shape of the curves of Figures 11 and 12. Differently, if the A/C changes the direction of motion, i.e. instead of moving forward, moves backward, during *push-back* manoeuvres for instance, there is the need to change the sign of the previous equations. For this reason, the RHS of (3) and (4) is multiplied by $(-\tanh(\tau \cdot V_x))$, where τ is a time constant chosen by the user and the tanh is used to assure a smooth transition around zero (the A/C is assumed to move forward when $V_x < 0$). The final equations are:

$$D = [\mu \cdot F_z + D' cos(\alpha_y) - S' sin(\alpha_y)] \cdot [-\tanh(\tau \cdot V_x)]$$

$$S = [S' cos(\alpha_y) + D' sin(\alpha_y)] \cdot [-\tanh(\tau \cdot V_x)]$$

The torque developed by the Self Aligning Torque can be simply computed using the look-up table of Figure 13. A snapshot of the tyre model in Dymola is given in Figure 14.

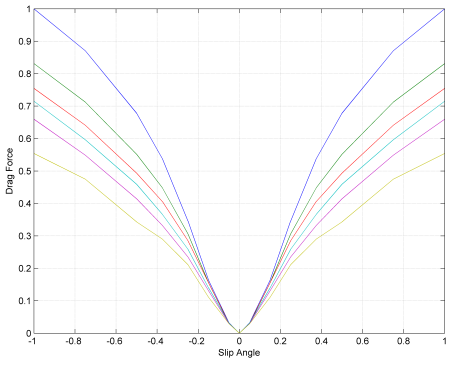

Figure 11: Drag Force vs. Slip Angle for different Vertical Load (Normalized)

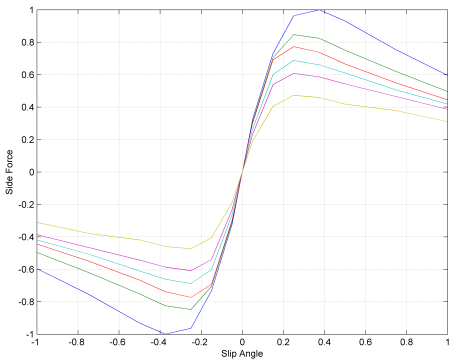

Figure 12: Side Force vs. Slip Angle for different Vertical Load (Normalized)

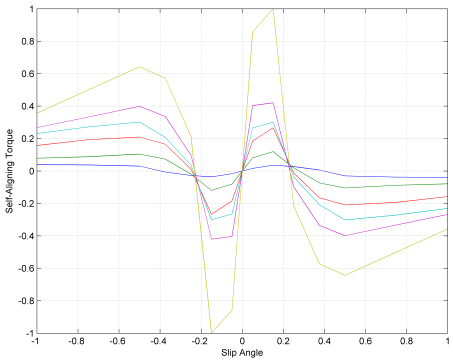

Figure 13: Self Aligning Torque vs. Slip Angle for different Vertical Load (Normalized)

2.5 Engine Model

The Engine Model is simply represented by a PID Controller. The user can define the desired steady state velocity and the spool time: the engine forces change accordingly to maintain the value of the demanded velocity. In fact during a turn, the A/C speed tends to decay because of the development of the centripetal force at the tyre contact footprint which counterbalances the centrifugal force. The user can also decide when to switch the engine on $(Thrust \neq 0)$ or off $(Thrust = 0)$ due to conditions linked either to time-based events or boolean-based events. Furthermore, in order to simulate an instantaneous loss of thrust, due for instance to an engine failure for the simulation of a rejected take-off case, the *TriggeredMax* block is used. It samples the continuous input signal whenever the trigger input signal is rising (i.e., trigger changes from false to true). The maximum, absolute value of the input signal (Engine Thrust) at the sampling point is provided as output signal. So the Thrust on the remaining functioning engines is assumed to be constant and its value equal

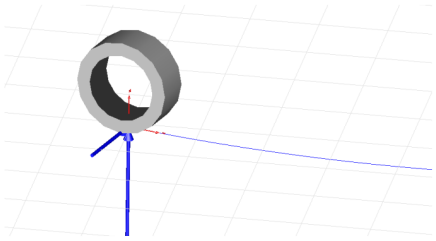

Figure 14: Tyre Model in Dymola

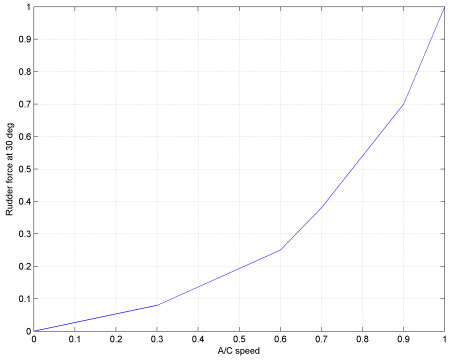

Figure 15: Rudder Force at 30° Rotation vs. A/C Speed (Normalized)

to the one at the instant when the failure occurred.

2.6 Aerodynamic Model

The Aerodynamic forces and momenta are lumped at the CG location. The equations used are as follows:

$$\begin{aligned} F_{x_A} &= \frac{1}{2}\rho V_{CG}^2 S\, C_x \\ F_{y_A} &= \frac{1}{2}\rho V_{CG}^2 S\, C_y \\ F_{z_A} &= \frac{1}{2}\rho V_{CG}^2 S\, C_z \\ M_{x_A} &= \frac{1}{2}\rho V_{CG}^2 S\, b\, C_l \\ M_{y_A} &= \frac{1}{2}\rho V_{CG}^2 S\, \bar{c}\, C_m \\ M_{z_A} &= \frac{1}{2}\rho V_{CG}^2 S\, b\, C_n \end{aligned} \tag{5}$$

where S is the wing wet area, b the wing span, and $\bar{c}$ the mean aerodynamic chord. These equations are multiplied with a positive or negative sign to account for the axes reference system. The computation of some of the angles necessary for the evaluation of the coefficients of (5) is as follow:

$$\alpha = \arctan\left(\frac{u}{w}\right) \qquad \beta = \arcsin\left(\frac{v}{|V_{CG}|}\right)$$

Other angles and their rate of change are computed using a similar approach.
The rotation of the Rudder is taken into account separately using the look-up table of Figure 15. It is assumed that the rudder has full authority when its rotation reaches 30°, and it increases linearly from zero to 30°. The rotation of the rudder implies also a rotation of the nose wheel, this has been implemented in the Steering Laws in the Monitoring and Commanding Model.

2.7 Hydraulics Steering System Model

The Hydraulics Steering System Model consists of a Nose Wheel Steering (NWS) and a BWS system. For the first one the kinematics of the actuation consists of a push-pull actuator arrangement which is capable to steer the A/C from a straight ahead position ($\theta_{NWS} = 0\ deg$) to a full powered steering rotation of the Nose Wheel ($\theta_{NWS} = \pm\theta_{NWS_{max}}$). For the second one, the kinematics consist of a single linear actuator, which steers the BWS accordingly to the actual position of the NWS angle and ground speed of the A/C ($\theta_{BWS} = f(\theta_{NWS}, GS_{A/C})$). An overview of the NWS and BWS Steering System models is given hereafter.

2.7.1 NWS Hydraulics Steering System Model

At the top-level, the system briefly consists of a Normal Selector Valve Manifold (NSELVM), an Alternate Selector Valve Manifold (ASELVM), a Local Electro-hydraulic Generation System (LHEGS), Nose Landing Gear (NLG) Shutoff-Swivel Valve, an Hydraulic Control Block (HCB), a servo-valve electro-hydraulic NWS, two Change Over Valves and two steering actuators. In addition, the system is connected to the hydraulic power distribution system via the High Pressure ($\approx 350\ bar$) and Low Pressure Manifolds ($\approx 5\ bar$). All the electrical signals necessary to energize and de-energize the various selector valves and command the servo-valve are sent by/to COM/MON to the Hydraulics System. In turn, the latter transmits all the signal necessary to monitor the system to COM/MON, for instance the value of the pressure downstream NSELVM, via Pressure Transducer (PT) PT4.
In the model, all the previous elements have been modeled, except the ASELVM and the LHEGS, which are

mainly necessary only if particular faults in the system occur (Reversion from Normal to Alternate Mode) and they will be modeled in the future, see Figure 16.

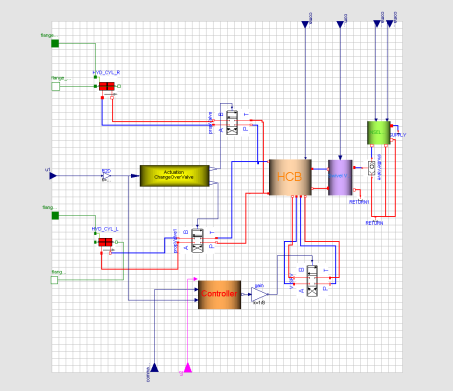

Figure 16: NWS Hydraulics Steering System Model in Dymola

The model of COM/MON does not pretend to be exhaustive nor representative of the whole COM/MON system, its principal task is to support the functioning of the Hydraulics System Model. The Model has been built keeping a net interface between the hydraulic domain, the mechanical domain and the avionic domain: the green flanges represent the interface with the attachment points of the mechanical steering actuators and the blue and purple signals the interface with the avionic domain, see Figure 16.

The position of the spool of the servo-valve is controlled by a PI controller which modulates the current in order to minimize the error between NWS commanded angle ($\theta_{NWS_{com}}$) and actual NWS angle (θ_{NWS}). The position of the servo-valve spool allows the hydraulic flow to differentially pressurize the four chambers (Left and Right, Annulus and Full Bore) of the steering actuators, so to create push or pull forces on the pistons ends.
The attachment points of the actuators are fixed: to the stationary flange for the cylinders and to the rotating sleeve for the pistons, respectively. This, and their position with respect to the upper strut of the shock absorber, are such to create a steering torque, which is transmitted, via the torque links, to the bottom of the shock absorber strut (piston fork) allowing the A/C to steer, see Figures 17, 18 and 19.
Of particular interest is the situation when one of the two actuators stalls: the line of action of the hydraulic force intersects the axle of rotation of the strut, creating no moment arm. The angle at which this happens is called *Change Over Angle* (θ_{COV}), and it is equal to:

$$\theta_{COV} = \theta_0 - \arctan(Fr_y/Fr_x)$$

with θ_0 being the angle between the x axis of the nose landing gear reference frame and the vector $\mathbf{S_rO_N}$, Fr_x and Fr_y equal to the x and y coordinates of Fr. These coordinates given in a reference system with the $x-y$ plane orthogonal to the strut axle (if the rake angle is different from zero).

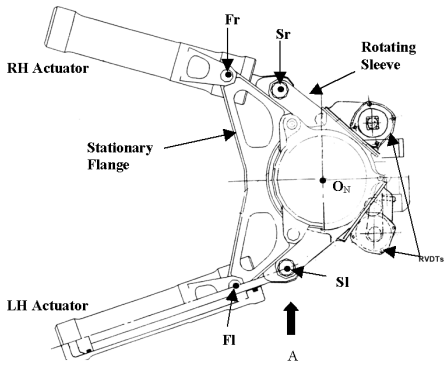

Figure 17: Actuators-rotary sleeve assembly

When $\theta_{NWS} = \pm\theta_{COV}$, one of the two Change Over Valve receives the command to change its position, see Figure 16, either the left or the right one depending if the A/C is performing a clockwise turn or counterclockwise turn, so that the corresponding actuator begins to push or pull and viceversa.

2.7.2 BWS Hydraulics Steering System Model

At the top-level, the system briefly consists of a Steering Selector Valve Manifold (SSELVM), a left and right BWS Hydraulic Control Block including Selector Valves and Steering Actuator, a left and right lock actuator, a left and right BWS electro-hydraulic servovale, an High Pressure supply line (HP) and Low Pressure supply line (LP) Manifolds and ATA 29 Electro-Motor Pump (EMP), see Figure 20.
Whilst the steering functions of the BWS is similar to the NWS, except the fact that there is one linear steering actuator per side, the additional challenge has been in modelling the lock/un-lock mechanism and un-lock actuator, as already explained in § 2.3.1, see Figure 8.

2.8 Monitoring and Commanding Model

The Monitoring and Commanding Model developed at this stage has the main purpose of allowing the correct functioning of the hydraulic and mechanical Model.

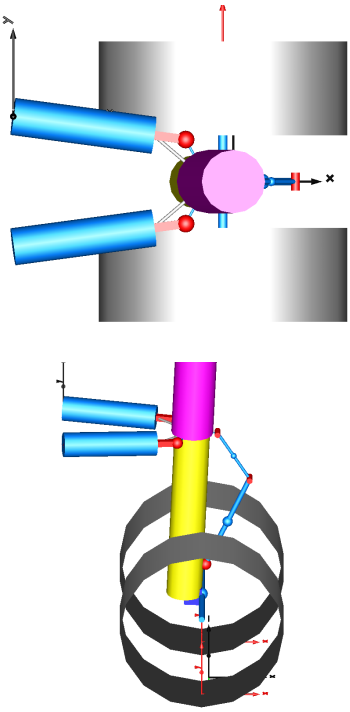

Figure 18: NLG Model with Actuators-rotary sleeve assembly in Dymola

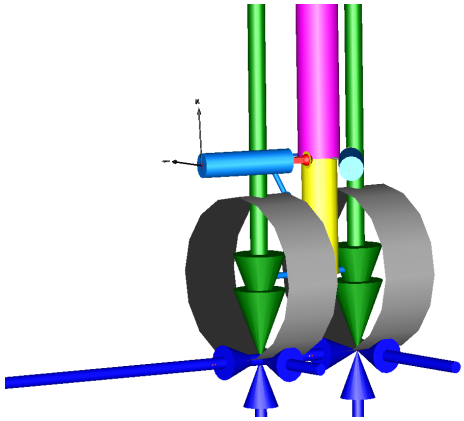

Figure 19: NLG driven by hydraulics actuators at 70° with side, drag and vertical forces (blue) and self-aligning torque (green) in Dymola

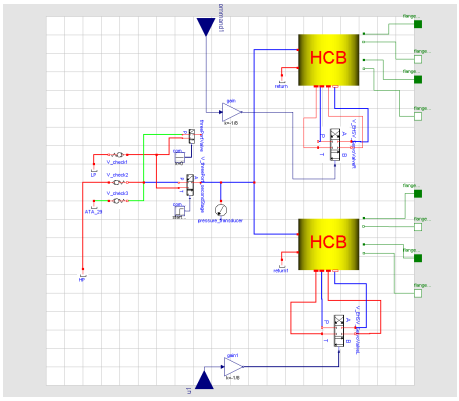

Figure 20: BWS Hydraulics Steering System Model in Dymola

The signals to energize or de-energize the several selector valves are sent accordingly to the actual conditions of the A/C, so to create a closed loop between the main three domains. The implementation of the Steering Laws has been also developed in this model, see for instance the command of the BWS angle in accordance with the actual NWS angle, Figure 21.
A more comprehensive model will be developed in a second stage: in doing that, an extensive use of the *StaeGraph* Library will be pursued.

3 Simulation Results

The following sections highlight the Dymola set up used to run simulations and the results obtained from a simulation of a Rejected Take Off (RTO) scenario.

3.1 Simulation Settings

The type of integration algorithm used depended upon the model that was tested. In the case of pure mechanical model, the *Dassl* or the *Lsodar* algorithms performed in an excellent manner. When it came to simulate the full model, combining avionic, hydraulic and mechanical domains, the best performance has been achieved using the *Sdirk34hw* method. Notably, the increase of tolerance of the integrator did not improve the simulation time: as explained in [2], a condition of optimum should exists, in the case of the full model a tolerance of 10^{-5} was used. Quite challenging has been the identification of the right initial conditions: Dymola by default, assigns arbitrary values for the initial conditions of certain variables. The assumption made by the software should always be validated by the user. In the case of the full A/C model, at the beginning of the simulation, there are many events that occur: the A/C is settling down on the soil (impact force different from zero and the shock absorber starts to be compressed), the A/C speed begins to reach the steady state value, and especially, the hydraulic circuit tends to find the steady state condition. All this could be quite time consuming from a simulation point of view. Ideally the user should try to find the value of the variables in the steady state condition which would like to use as starting point of his/her investigation, record those values, and use them as initial conditions for all the following simulations. When this is done, he/she

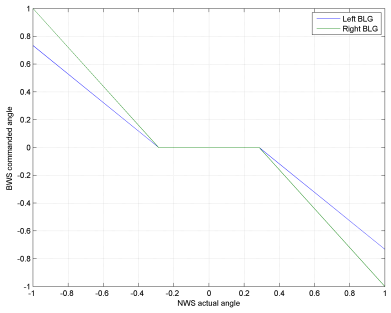

Figure 21: BWS Steering Laws

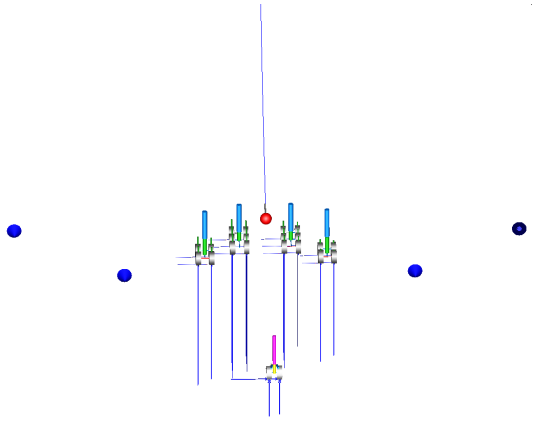

Figure 22: Snapshot of the A/C, five seconds after a left outer engine failure with highlighted CG trajectory (in blue)

could simulate the model up to the steady state condition and then used this final condition, as a starting point for a new simulation. This method can be used only if the model has reached an high level of maturity and many changes are no longer necessary.

3.2 RTO simulation test

The test has been carried out with the following preconditions and assumptions: A/C speed at the instant of the left outer engine failure equal to 130 kt, mass equal to 560 t, CG position equal to 37.5 %, rolling friction coefficient μ_R, equal to 6 e^{-3}, all the steering controllers active, ($\theta_{NWS_{com}} = 0$) with no pilots correction after engine failure, no aerodynamic forces and rudder force.
The main outputs of interest are the trajectory of the nose and CG, Figures 23 and 24, A/C heading ψ, Figure 27; A/C CG lateral linear and angular accelerations, $a_{y_{CG}}$ and $\dot{\omega}_{z_{CG}}$ respectively, Figures 25 and 26.
Notably, It takes 1.25 s before the CG linear acceleration along y direction starts to become negative, see Figure 25, in fact the CG first moves towards the positive $x-z$ half plane and then after a while, it starts to move towards the negative $x-z$ half plane, following the nose. After three seconds from the instant of the simulated engine failure, the nose has moved of circa 37.22 cm towards the left.

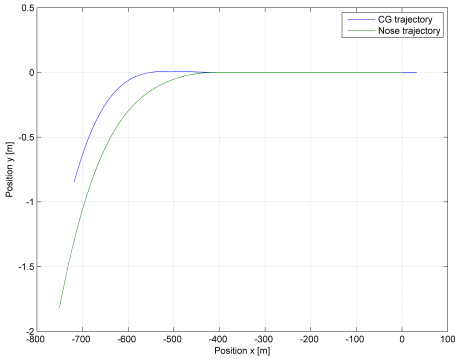

Figure 23: CG and Nose trajectory (engine failure at $x = -382.47$ m. A/C moves forward when $x < 0$)

4 Future Work

The future work will be mainly based on the enhancement of the Aircraft Library with the development of more comprehensive models and new models as well; on the investigation of Modelica capability to produce code to run models in a Real Time environment for hybrid simulations on the landing gear test rig and, finally, on the validation of the models with Flight Test and Test Rig Data.

5 Conclusions

Though the work presented in this paper is one of the first large-scale application of Modelica for the simulation of landing gears and aircrafts, its findings made clear the power and potentiality of the language to model and simulate so tightly coupled systems such the ones which equip new modern airplanes.
The fact that the source code is completely open to the user implies a huge potentiality to increase the level of accuracy of every model component/assembly/system. The acasuality feature of the language implies a real opportunity to develop a re-usable library of models which is not truly possible with models built with a casual language. Furthermore, the system modeled with Modelica provides a unique feature which is the capability of the model to *look like* the real system undergoing the design process: in a large enterprise this

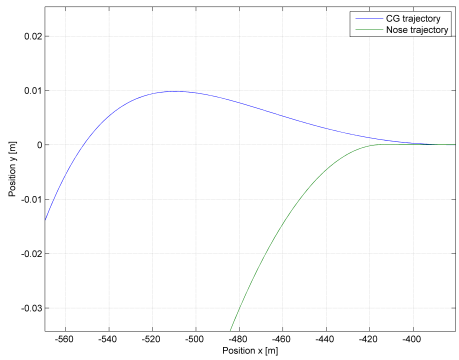

Figure 24: CG and Nose trajectory (engine failure at $x = -382.47\ m$. A/C moves forward when $x < 0$) (Magnified)

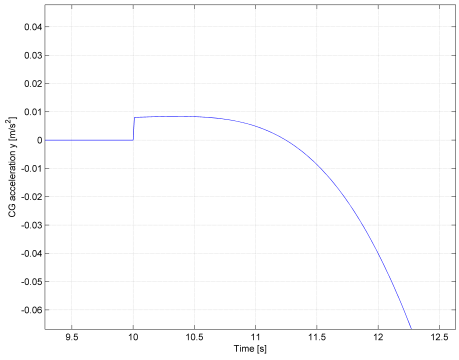

Figure 25: A/C linear acceleration along y at CG location (Magnified)

represents a *point of convergence* between designers and modelers. No particular skills are necessary to be able to *read* the model which faithfully should represent the system, so that feedbacks, critics, enhancements, approvals can be easily agreed between several actors not necessarily experts of modelling and simulations techniques, even before any type of simulation is performed.

If Modelica is used in a large industrial environment some enhancements are advisable, though these issues may not be necessarily attributable to Modelica itself: the capability of creating geometry (with mass, inertia, CG location and surface shape information) directly from a Computer-Aided Drawing (CAD) software in an automated manner; a flexible body simulation capability, including contacts and conditional connection/dis-connection of bodies/joints during the same simulation.

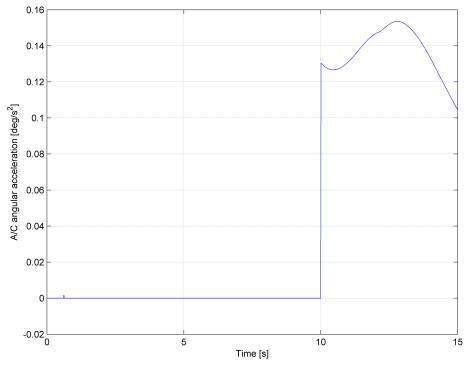

Figure 26: A/C angular acceleration along z at CG location

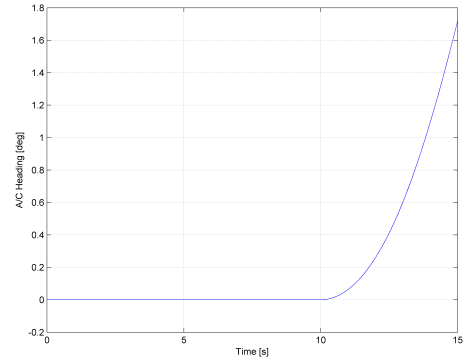

Figure 27: A/C heading angle ψ

6 Acknowledgments

The Author would like to acknowledge Airbus for giving the opportunity to attend the Modelica 2008 Conference and present this work, Mr. Sanjiv Sharma for the continuous support and for reviewing the paper, Miss. Serena Simoni for having accepted the challenge of learning Modelica and Dymola and started this work and finally Claytex Services Limited and Dynasym AB for solving technical issues related to the use of the software.

Acronyms

A/C Aircraft

ASELVM Alternate Selector Valve Manifold

BLG Body Landing Gear

BWS Body Wheel Steering

CAD Computer-Aided Drawing

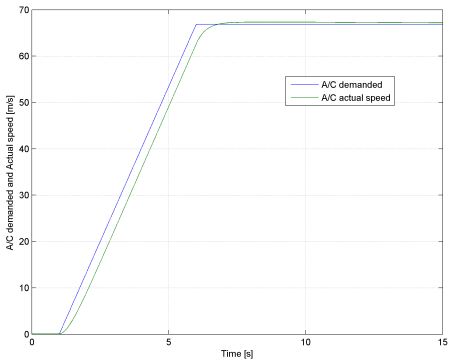

Figure 28: A/C demanded and actual speed [m/s]

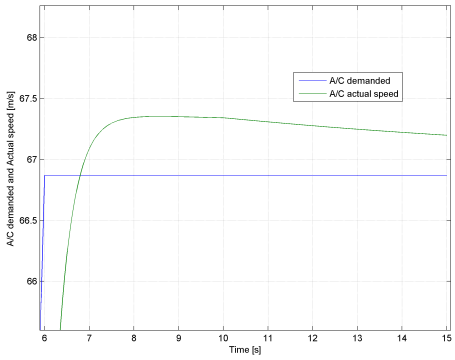

Figure 29: A/C demanded and actual speed [m/s] (Magnified)

CG Centre of Gravity

EMP ATA 29 Electro-Motor Pump

GUI Graphical User Interface

HCB Hydraulic Control Block

HP High Pressure supply line

LHEGS Local Electro-hydraulic Generation System

LP Low Pressure supply line

MAC Mean Aerodynamic Chord

NLG Nose Landing Gear

NSELVM Normal Selector Valve Manifold

NWS Nose Wheel Steering

PT Pressure Transducer

RTO Rejected Take Off

References

[1] M. Beckman and J. Andreasson. Wheel model library for use in vehicle dynamics studies. KTH Vehicle Dynamics, Sweden
mb.johang@fkt.kth.se

[2] C. Clauβ and P. Beater. Electronic, Hydraulic, and Mechanical Subsystems of a Universal Testing Machine Modeled with Modelica. 2nd International Modelica Conference, Proceedings, pp. 25-30, Germany